



Subscriber access provided by University of Minnesota Libraries

**Article** 

# On the Economics and Process Design of Renewable Butadiene from Biomass-Derived Furfural

Anatoliy Kuznetsov, Gaurav Kumar, M. Alexander Ardagh, Michael Tsapatsis, Qi Zhang, and Paul J. Dauenhauer

ACS Sustainable Chem. Eng., Just Accepted Manuscript • DOI: 10.1021/acssuschemeng.9b06881 • Publication Date (Web): 05 Feb 2020

Downloaded from pubs.acs.org on February 10, 2020

### **Just Accepted**

"Just Accepted" manuscripts have been peer-reviewed and accepted for publication. They are posted online prior to technical editing, formatting for publication and author proofing. The American Chemical Society provides "Just Accepted" as a service to the research community to expedite the dissemination of scientific material as soon as possible after acceptance. "Just Accepted" manuscripts appear in full in PDF format accompanied by an HTML abstract. "Just Accepted" manuscripts have been fully peer reviewed, but should not be considered the official version of record. They are citable by the Digital Object Identifier (DOI®). "Just Accepted" is an optional service offered to authors. Therefore, the "Just Accepted" Web site may not include all articles that will be published in the journal. After a manuscript is technically edited and formatted, it will be removed from the "Just Accepted" Web site and published as an ASAP article. Note that technical editing may introduce minor changes to the manuscript text and/or graphics which could affect content, and all legal disclaimers and ethical guidelines that apply to the journal pertain. ACS cannot be held responsible for errors or consequences arising from the use of information contained in these "Just Accepted" manuscripts.

## On the Economics and Process Design of Renewable Butadiene from Biomass-Derived Furfural

Anatoliy Kuznetsov<sup>1,2</sup>, Gaurav Kumar<sup>1,2</sup>, M. Alexander Ardagh<sup>1</sup>, Michael Tsapatsis<sup>3,4</sup>, Qi Zhang<sup>1</sup>, Paul J. Dauenhauer<sup>1,2</sup>\*

- 1. University of Minnesota, Department of Chemical Engineering and Materials Science, 421 Washington Ave. SE, Minneapolis, MN 55455
- 2. Center for Sustainable Polymers, University of Minnesota, 207 Pleasant Street SE, Minneapolis, MN 55455
- 3. Department of Chemical and Biomolecular Engineering & Institute for NanoBioTechnology, Johns Hopkins University, 3400 N. Charles Street, Baltimore, MD 21218.
- 4. Johns Hopkins University, Applied Physics Laboratory, 11100 Johns Hopkins Road, Laurel, MD 20723

Keywords: Butadiene, Biomass, Furfural, Process, Economics

**Synopsis.** A renewable process to manufacture butadiene from furfural using acid-catalyzed dehydradecyclization of tetrahydrofuran is analyzed for economic viability.

**Abstract.** The catalytic conversion of biomass-derived furfural to 1,3-butadiene is a potential synthetic route to renewable rubber. In this work, we present and evaluate a conceptual process design consisting of three steps: (i) decarbonylation of furfural to furan, (ii) hydrogenation of furan to tetrahydrofuran, and (iii) dehydra-decyclization of tetrahydrofuran to 1,3-butadiene. Detailed reaction and separation systems are designed using process simulation and economic optimization. At a scale of 77 kton yr<sup>-1</sup> of furfural (100 kmol hr<sup>-1</sup>) purchased at \$1.84 kg<sup>-1</sup> (\$176 kmol<sup>-1</sup>), a minimum sale price of butadiene of \$5.43 kg<sup>-1</sup> is calculated. The selectivities of the decarbonylation and dehydra-decyclization catalysts are identified as the key process parameters by performing a sensitivity analysis on the minimum selling price of butadiene. Economic and technological factors necessary to achieve a minimum sale price of butadiene below \$1.50 kg<sup>-1</sup> (\$81 kmol<sup>-1</sup>) are identified. A quantitative treatment of process sustainability results in a carbon efficiency of ~58% and an E-factor of ~1.5 for the overall process.

<sup>\*</sup>Corresponding Author: hauer@umn.edu

**Introduction.** The sustainability of the global economy depends on the affordability of sustainable polymeric materials, which necessitates economically competitive sustainable monomer manufacturing.<sup>2</sup> The synthesis of industrially important monomers such as C5 olefins, p-xylene, and acrylonitrile from biomass-derived feedstocks has already been demonstrated.<sup>3–8</sup> 1,3-Butadiene is another monomer whose synthesis from biomass has attracted recent interest, owing to its applications in products such as tires and sealants.<sup>9,10</sup> Traditionally, butadiene has been produced via the dehydrogenation of *n*-butane, <sup>11</sup> or as a byproduct of ethylene production during naphtha cracking. 12,13 To date, proposed biomass-based synthesis routes for butadiene have generally included either ethanol or C4 diols as starting materials. 12,14,15 Ipatieff and co-workers proposed the dehydrogenation of ethanol to acetaldehyde, followed by condensation and deoxygenation to butadiene. 12,16,17 and butadiene selectivities of 60-70% have been achieved with this approach at moderately high ethanol conversions (60-75%). Lebedev developed a direct synthesis of butadiene from ethanol. 18 leading to a butadiene yield of ~65% at high ethanol conversions (~88%) on promoted tantalum-containing zeolites. 19 As already mentioned, the dehydration of C4 diols including 1,3butanediol (1,3-BDO), 14,20,21 2,3-butanediol (2,3-BDO), 14,22-25 and 1,4-butanediol (1,4-BDO), 14,26 to butadiene has also received attention since these alcohols can be derived from glucose via fermentation pathways. <sup>27,28</sup> Song et al. have recently reported the economic feasibility of butadiene production from 2,3-BDO using amorphous calcium phosphate (ACP)/ hydroxyapatite-alumina catalysts.<sup>29–31</sup> At the scale of 2500 kg/h feed (2,3-BDO) assumed to be purchased at \$0.8/kg, the butadiene price was estimated to be \$1.62/kg.<sup>30</sup> The price point for butadiene was found to be sensitive to 2,3-BDO prices, and payback times of less than five years were only possible for 2,3-BDO prices below \$1.3/kg.<sup>30</sup>

While a stand-alone process utilizing furfural directly as a feedstock has not been utilized to the best of our knowledge, Athaley *et al.* have recently reported the production of butadiene from furfural as a byproduct in p-xylene. The proposed biorefinery utilizes biomass purchased at \$0.06/kg at a process scale of ~400 kT feed/year to produce ~81 kT p-xylene/year and ~64 kT furfural/year to propose a butadiene minimum selling price (MSP) of \$1.3 /kg.<sup>32</sup> In this work, we propose and evaluate an envisioned industrial process to produce butadiene from furfural via tetrahydrofuran (THF), with the goal of identifying key opportunities for technological advancement which could make this pathway commercially viable. Although the process is not profitable given current prices, we assess the furfural and butadiene prices that might lead to economic viability. Furan derivatives have been studied as a biomass-derived feedstock both for fuels and for commodity chemicals, and furfural yields of 72-87% from corn-derived feedstock including glucose and fructose have been achieved.<sup>33-41</sup> The promising nature of furfural as a biomass-derived value-added chemical has led to significant technological improvements in its manufacture, <sup>42,43</sup> and global production is projected to grow, particularly in China.<sup>44</sup> This market growth is primarily driven by a demand for furfuryl alcohol, which is used in foundry resins.<sup>42</sup> Since the production of furfuryl alcohol

from furfural is industrially practiced, one commercially viable alternative of producing butadiene from furfural would be designing supported metal catalysts which produce both furfuryl alcohol and furan in appreciable amounts. In such a scenario, furan can be converted to butadiene, and the primary side product (furfuryl alcohol) can be directly sold. While this alternative can potentially offset some costs possibly improving the overall process economics, this assessment is not straightforward. The separation of furfuryl alcohol from unreacted furfural is difficult, and the distillation sequence required to purify furfuryl alcohol in such a process would be relatively expensive. Moreover, Bhogeswararao *et al.* have only reported comparable furfuryl alcohol and furan selectivities on a Pd catalyst at hydrogen pressures of 20 bar, which would incur significant compression costs. Resasco and co-workers have demonstrated comparable furfuryl alcohol and furan selectivities on a Ni/SiO<sub>2</sub> catalyst at ambient pressure, but the product distribution (including tetrahydrofurfuryl alcohol, butanal, butane, butanol, and methylfuran in significant amounts) is different enough from that given by a Pd catalyst to warrant a new, separate process design with different separation sequences. Consequently, we do not consider the sale of furfuryl alcohol in our process design in the current work.

The direct transformation of furfural to THF involves simultaneous decarbonylation and hydrogenation. <sup>26,47–49</sup> However, the highest selectivity achieved under continuous-flow conditions has remained low (<40%), and the presence of side products (e.g. tetrahydrofurfuryl alcohol, furan, furfuryl alcohol, butanol, etc.) would likely lead to high downstream separations cost. <sup>36–38</sup> Instead, we consider a two-step process sequence from furfural to THF, with furan as an intermediate. The first step in the proposed process is the decarbonylation of furfural to furan, shown in **Scheme 1**. This reaction can take place in the gas or liquid phases, and supported Pd catalysts are usually used to achieve high yields. <sup>50–53</sup> Although the catalyst is prone to coking, <sup>53</sup> the co-feeding of hydrogen mitigates deactivation by hydrogenating and/or inhibiting the formation of coking precursors *in situ*, <sup>44</sup> and cumulative furan site-time yields as high as 100 kg per g Pd have been recently achieved. <sup>53</sup> While comparable furan yields have been reported on platinum, <sup>54</sup> the reaction is particularly sensitive to Pt particle size/shape, <sup>55</sup> and the choice of support. <sup>56</sup> For this work, we consider the gas-phase decarbonylation of furfural with a Pd/alumina catalyst treated with cesium carbonate, which has been reported to give >98% furan selectivity at >90% furfural conversion, being stable for ~383 hours on-stream before regeneration in examples 1-2 by Li and Ozer *et al.*. <sup>53</sup>

The subsequent step to decarbonylation is the hydrogenation of furan to THF. Platinum,<sup>57</sup> ruthenium,<sup>58</sup> and palladium<sup>59</sup> have all been used as heterogeneous catalysts for this reaction. Hydrogen pressures of 7-35 atm and reaction temperatures of 80-150 °C are typically used.<sup>60,61</sup> While Raney nickel is often used,<sup>61</sup> palladium offers higher THF selectivity.<sup>59</sup> We consider a bubble-column reactor in which

hydrogen at 22.5 bar is bubbled through liquid furan on a 5% Pd/carbon catalyst; these conditions have been shown to give nearly quantitative yields of THF at complete furan conversion.<sup>59</sup>

The third and final step is the dehydra-decyclization of THF to butadiene. The major side products in this reaction are propene and formaldehyde (Retro-Prins condensation products),<sup>62</sup> butenes, and heavy organics (C6+ fraction); while traditional solid acids like aluminosilicate zeolites are active, butadiene selectivities remain low (~50-60%) across all THF conversions.<sup>63</sup> We have previously reported that aluminum-free phosphorus-containing siliceous self-pillared pentasil (P-SPP) zeolite exhibits ~87% butadiene selectivity at ~83% THF conversion at 400 °C, albeit at a very low space velocity (0.04 g THF gcat<sup>-1</sup> hr<sup>-1</sup>) owing to its low reactivity.<sup>63</sup> For this work, we conducted experiments on P-SPP at 425 °C and used the obtained conversions and product selectivities in the simulation of this step.

In total, the proposed process comprises the conversion of furfural to furan in a packed-bed reactor, the purification of furan using distillation, the hydrogenation of furan in a high-pressure bubble-column reactor to THF, the dehydra-decyclization of THF to butadiene in a packed-bed reactor, and the purification of butadiene using distillation followed by absorption (**Scheme 1**). Process simulation and optimization are used to develop a detailed process design, and a techno-economic analysis assesses economic viability and provides targets for future research.

**Methods.** The conceptual design of a process to convert furfural to butadiene via THF was developed to assess the industrial feasibility of this synthetic route. The process comprises three stages, as shown in **Figure 1**: (1) decarbonylation of furfural to furan and carbon monoxide, along with the associated separations and recycle, (2) furan hydrogenation to THF, and (3) dehydra-decyclization of THF to butadiene followed by butadiene purification. Aspen Plus (V8.6 Aspen Technology) was used with the non-random two-liquid (NRTL) activity coefficient model and the Redlich-Kwong equation of state to simulate the proposed process. The simulation included the Heater, HeatX, RStoic, RadFrac, Flash2, Compr, Sep2, Pump, and Extract modules. The power rating and cost of all major equipment, as well as stream flow rates, temperatures, and pressures, are included in Sections 1-2 of the **Supporting Information**. Aspen Economic Analyzer was used to estimate capital and operating costs (except for process sections described in Section 9 of the **Supporting Information**) and Microsoft Excel was used for economic analysis.

Capital and operating costs for the proposed process were determined using the Aspen Process Economic Analyzer (V8.6 Aspen Technology) in 2013 USD and indexed to the year 2018 using the Chemical Engineering Plant Cost Index.<sup>64</sup> It is assumed that the plant will be constructed as a greenfield facility with access to external utilities (US Gulf coast); therefore, the costs of equipment such as a wastewater treatment unit and storage tanks for feedstocks and products were considered. Catalyst synthesis costs were estimated using CatCost (V1.0.0 NREL); details can be found in Section 8 of the **Supporting** 

**Information**. A 30-year plant lifetime was considered for the proposed process at a scale of 100 kmol hr<sup>-1</sup> (77 kton yr<sup>-1</sup>) of furfural processed and 73 kmol hr<sup>-1</sup> (32 kton yr<sup>-1</sup>) of butadiene produced. An economic analysis was conducted to determine the minimum selling price (MSP) of butadiene at which the proposed process would be profitable. Important economic parameters included a 10% minimum annual rate of return (MARR), a 35% tax rate, and a 30-year project lifetime; additional details are given in Section 3 of the **Supporting Information**.

Furfural decarbonylation. As shown in Figure 1, the process feed consists of furfural and hydrogen. The gas-phase decarbonylation of furfural to furan and carbon monoxide is performed at 280 °C and ambient pressure with a 0.5 wt.% Pd/alumina catalyst in a fixed-bed configuration.<sup>53</sup> Hydrogen is co-fed in a 2:1 molar ratio with furfural (stream 2) to mitigate catalyst deactivation due to coke buildup. 44,53 A furfural consumption rate of  $5.80 \times 10^{-3}$  mol furfural gcat<sup>-1</sup> hr<sup>-1</sup> with 98% selectivity to furan, 1% selectivity to furfuryl alcohol, 0.5% selectivity to THF, and 0.5% selectivity to 2-methylfuran at 95% furfural conversion is chosen based on values reported by Li et al..<sup>53</sup> It is assumed that coke buildup, rather than sintering, was the primary pathway for catalyst deactivation; the temperature in reactor R-1 is significantly lower than the Hüttig temperature of palladium, so the Pd clusters can be assumed sufficiently immobile.<sup>65</sup> Therefore. the total lifetime of the catalyst is estimated as five years based on typical values for palladium hydrogenation catalysts.<sup>65</sup> We note that the possibly detrimental effects of inorganic impurities and salts inherently present in biomass-derived feed streams has not been accounted for in the catalyst lifetime estimation. During plant operation, two parallel reactors would be employed for furfural decarbonylation, and the catalyst would be regenerated with steam and air at 350 °C.53 Only one of each reactor is shown in Figure 1 for brevity, but costs are calculated using two reactors for each of the process sections to allow for continuous production; see Section 8 of the Supporting Information for details. The effluent from reactor R-1 (stream 3) is used to preheat the reactor feed (stream 1) and then sent (stream 4) to distillation column D-1.

The bottoms of column D-1 (stream 9), containing unreacted furfural as well as furfuryl alcohol, are sent to distillation column D-2, which removes 88% of the furfuryl alcohol as well as 46% of the remaining furfural. The possibility of column fouling resulting from the polymerization of some of these species, and the resulting cleaning downtimes has not been considered in this work. The bottoms of column D-2 (stream 11) are purged, and the distillate (stream 10) is recycled to reactor R-1. The distillate of column D-1 (stream 5), containing furan, hydrogen, and carbon monoxide, is sent to flash tank F-1, which separates the furan from the permanent gases. The gases (stream 6) are compressed to 35 barg and used to preheat the furan feed to reactor R-2. After further cooling to 60 °C, the gases are sent to a two-stage cellulose acetate membrane module, which has been shown to produce a permeate of 97 mol% hydrogen at 4.5 barg and a reject of 98% carbon monoxide from a feed gas of 52% hydrogen. The permeate (stream 8) is

recycled to reactor R-1, and the reject (stream 7) is sent to a carbon monoxide boiler operating at 1400 °F,<sup>67</sup> which generates 100 psia steam; for details, see Section 9 of the **Supporting Information**.

**Furan hydrogenation.** The liquid furan from flash tank F-1 (stream 12) is preheated by the compressed vapor and then sent to pump P-1, which provides a discharge pressure of 22.5 bar. The furan is then fed to reactor R-2, which operates as a three-phase bubble-column reactor to maximize mass transfer.<sup>68</sup> At the operating conditions of 100 °C and 22.5 bar, a 5 wt.% Pd/carbon catalyst has been shown to achieve a reaction rate of 1.12 mol gcat<sup>-1</sup> hr<sup>-1</sup> at quantitative (100%) conversion.<sup>59</sup> Since hydrogen (stream 13) is fed to the reactor stoichiometrically, the quantitative conversion of furan makes a recycle loop unnecessary. A catalyst lifetime of five years is again selected as a representative value for Pd as hydrogenation catalysts.<sup>65</sup>

**THF Dehydra-Decyclization.** THF from reactor R-2 (stream 14) is fed to reactor R-3, where it undergoes a dehydra-decyclization reaction at 425 °C to form 1,3-butadiene and water as the major products. Although P-SPP is highly selective to butadiene, the low overall THF consumption rate on this material has been previously reported by Abdelrahman et al.<sup>63</sup> Using a lab scale fixed-bed flow reactor, we measured a THF consumption rate of 1.03 × 10<sup>-3</sup> mol THF gcat<sup>-1</sup> hr<sup>-1</sup> at a weight hourly space velocity of 0.09 g THF gcat<sup>-1</sup> <sup>1</sup> hr<sup>-1</sup> on P-SPP (Si/P=27). The obtained THF conversion (80.5%), as well as the selectivities (%C) to butadiene (81%), propene (1.4%), butenes (4.8%), and heavy organics (12.8%) were directly used in the simulation (reaction details can be found in Section 7.4 of the **Supporting Information**). While a mixture of 1-butene, 2-butene, and isobutene are observed experimentally, the boiling point of 1-butene is closest to that of 1,3-butadiene, and hence the process is simulated using the entire butene fraction as 1-butene, resulting in an overdesign of the downstream distillation column D-3 and the absorption column A-1. The online lifetime of the catalyst is estimated as 24 h based on previous 3-methyl-tetrahydrofuran dehydradecyclization experiments in the same packed-bed flow configuration conducted at 325°C. 7,69 It is likely that higher temperatures lead to faster deactivation rates due to rapid polymerization of butadiene, and the catalyst lifetime was also validated for these high temperature conditions; 24 hours was found to be a reasonable approximation (for details, see Section 7.4 of the Supporting Information). The catalyst deactivates through coke formation and can be regenerated through calcination in air at 550 °C for 12 h. 7,65 To allow for plant operation during regeneration, two parallel reactors are employed. The overall on-stream lifetime of the catalyst is estimated to be three months, meaning both catalyst charges would be replaced every six months.

The effluent from reactor R-3 (stream 16) is used to preheat the reactor feed and is then sent to distillation column D-3. The bottoms (stream 22) contain unreacted THF, as well as water and heavy impurities, and are sent to distillation column D-4, which separates the THF (stream 23) from the waste

(stream 24). The distillate of column D-3, containing propene, 1-butene, and 1,3-butadiene, is sent to an absorption column for purification. An absorption column (A-1) is chosen for the separation due to the close boiling points of 1-butene and 1,3-butadiene. An aqueous solvent (stream 20) selectively dissolves 1-butene and propene,<sup>70–72</sup> and the spent solvent (stream 21) is sent to wastewater purification; for details on wastewater treatment cost calculations, see Section 9 of the **Supporting Information**. The product butadiene stream (stream 19) is purified to 99.5 mol%, which is sufficiently pure for polymerization.<sup>73</sup>

#### Results and Discussion.

Capital and Operating Costs. Table 1 depicts the feedstock, product, and utility prices for the simulated process. For the base case design, the total capital investment is \$61.5 million, which includes equipment and installation costs, synthesis costs of the initial catalyst charges, and engineering and contingency costs. The most expensive section of the plant is the furfural decarbonylation, with a total capital investment of \$39.6 million, of which the distillation columns D-1 and D-2 account for \$27.4 million, due to the high flow rates in the recycle loop. The yearly operating cost is \$23 million, of which utilities account for \$16.6 million. Of the \$12 million annual utility cost associated with the furfural decarbonylation section of the plant, the distillation column D-1 accounts for \$10 million and the compressor C-1 accounts for \$0.9 million; this is due to the large recycle loop and the high pressure needed for the gas membrane separation. Due to the high separation costs associated with this section of the process, Aspen's optimization functionality was used to find the economically optimal condenser duties for columns D-1 and D-2. Although reactor R-2 operates at 22.5 bar, it is assumed that hydrogen is stored above this pressure, <sup>74</sup> and furan is pumped in the liquid phase before being heated, so there are no compression costs associated with the furan hydrogenation and the yearly utility cost of this section is only \$10,000.

**Butadiene Purification Sequence.** The high purity requirements (99.5 mol%) for the butadiene product and the 4.8% selectivity to butenes (simulated as 1-butene as mentioned in **Section 2.3**) in reactor R-3 make the purification of butadiene via distillation economically infeasible due to the similarity in boiling points (-4.4 °C for butadiene and -6.3 °C for 1-butene). A distillation column (D-3) is first used to separate butadiene and the lighter-boiling products (1-butene and propene) from THF (b.p. 66 °C), water, and the heavy impurities. This allows for a straightforward separation of THF from the waste stream as the distillate of column D-4, and also provides a 90 mol% butadiene distillate stream (stream 18). The absorption column A-1 is then used to purify the butadiene stream to 99.5 mol% with only a 3.3% loss of product. The wastewater purification required to recycle the spent solvent in stream 21 contributes a yearly cost of \$1.3 million, only 6% of the total plant operating cost.

Minimum Selling Price of Butadiene. The discounted cash flow method was used to calculate the minimum selling price (MSP) of butadiene that would yield a zero net present value for the entire project. For the base case process at a scale of 77 kton yr<sup>-1</sup> (100 kmol hr<sup>-1</sup>), the MSP of butadiene was calculated to be \$5.43 kg<sup>-1</sup>. As noted, this MSP is significantly higher than the one proposed by Athaley *et al.* in the combined biorefinery process producing p-xylene and butadiene, although the choice of catalysts for each of the three chemistries is identical as this work.<sup>32</sup> However, there are major differences in these two investigations in terms of the process scales considered to evaluate economics (400 kT /year vs. 77 kT/year), feedstock identity (raw biomass vs. furfural), butadiene stream purity (99% vs. >99.5%), and the complexity of the overall process (3 reactors, 2 distillation columns vs. 6 reactors, 4 distillation columns + 1 absorber). It is therefore unsurprising that our butadiene MSP is significantly higher than the one calculated by Athaley and co-workers.

The contribution of each section of the process to the MSP is shown in **Figure 2**. The feedstock cost, the labor and maintenance cost, and the capital and utility costs of each process section are labeled by color. The furfural feedstock is by far the largest contributor to the MSP of butadiene, accounting for \$4.50 kg<sup>-1</sup>, or 83% of the total project costs over the 30-year lifetime. This is due to a maximum theoretical yield for the process of 1 mole of butadiene per mole of furfural, and the current furfural price of \$1.84 kg<sup>-1</sup> (\$0.177 mol<sup>-1</sup>) would require a minimum butadiene price of \$3.27 kg<sup>-1</sup> (\$0.177 mol<sup>-1</sup>) to break even without considering any processing costs or material losses. However, the overall molar yield of butadiene in the base case process is only 73%, which further adds to the cost. The labor and maintenance, capital, and utility costs together contribute only \$0.80 kg<sup>-1</sup> to the MSP of butadiene. Possible scenarios discussing economic viability of the process subject to various technological and market factors are discussed in **Section 3.4.3**.

Sensitivity to Process Parameters. A sensitivity analysis was performed to determine the relative importance of various process parameters to the MSP of butadiene. Individual parameters were varied by ±10% of their base-case value while all remaining parameters were held constant and the MSP of butadiene was recalculated for each scenario. In the scenarios with varying plant size, the process was simulated at the new size and the MSP was recalculated based on the simulation results and is shown in Figure 3. The purchase price of furfural is the most important factor in the MSP of butadiene; a 10% change in the purchase price results in a 8.2% change in the MSP, which is consistent with the results shown in Figure 2. The only other factor which effected an MSP change of more than \$0.05 kg<sup>-1</sup> was the increase in plant size to 84 kton yr<sup>-1</sup> (110 kmol hr<sup>-1</sup>), suggesting that economies of scale may have an impact on processing costs; for details, see Section 6 of the Supporting Information. The hydrogenation catalyst for reactor R-1 is the most expensive catalyst due to the large mass of palladium required, but a 10% change in its cost

led to less than a \$0.01 kg<sup>-1</sup> change in the butadiene MSP. It is clear that the single most important factor in the economic viability of the process is the feedstock purchase price. We therefore devote the remainder of this work to examining the conditions under which the proposed process may be profitable.

**Reactor R-1 Performance.** 70% of the total operating cost is associated with the downstream separations and recycle of reactor R-1. There has been recent interest in developing a process-scale one-step synthesis of THF from furfural 36-38 as part of a biomass-to-solvent process. Under continuous flow conditions, a maximum selectivity of 41% at 100% conversion has been achieved with tetrahydrofurfuryl alcohol as the principal side product.<sup>47</sup> although Luque et al. report 80% THF selectivity at >90% furfural conversion in a batch microwave reactor with 30-minute residence time, with furan as the principal side product.<sup>49</sup> To assess the potential impact of research in this area on the operating costs of the proposed furfural-tobutadiene process, we considered a scenario with 95% selectivity to THF at full furfural conversion with furan as the only side product at atmospheric pressure and 423 K, which are similar conditions to those reported by Suarez et al.<sup>47</sup> In this scenario, the separations downstream of reactor R-1 would be considerably simplified, as shown in Figure 4. Hydrogen could be fed in a 1.9:1 molar ratio with furfural so that the reactor effluent would be composed only of furan, THF, and carbon monoxide. The vapor stream leaving flash tank F-1 would contain nearly pure carbon monoxide and would be sent to a furnace as described earlier.<sup>67</sup> The liquid stream would consist primarily of furan and THF, which would be separated by distillation column D-1 in Figure 4. The distillate, containing 33 mol% carbon monoxide, would continue to flash tank F-2 followed by reactor R-2, while the bottoms, containing practically pure THF, would be sent directly to reactor R-3. The process was simulated with these changes and the MSP of butadiene in this scenario was calculated to be \$4.74 kg<sup>-1</sup>, a 13% decrease from the base case.

Reactor R-3 Performance. The dehydra-decyclization stage of the process accounts for an additional 28% of the total base-case operating cost, of which 25% is from wastewater treatment of streams 21 and 24. Stream 24 removes heavy impurities and the water generated from the dehydra-decyclization reaction from the process, and stream 21 is spent solvent used to separate light impurities from butadiene. Since the cost of wastewater treatment depends on the quantity of organics to be removed, improved selectivity in reactor R-3 should decrease wastewater treatment costs. Analogously to the scenario with reactor R-1, we considered a catalyst which achieves 95% selectivity to butadiene at full THF conversion with heavy impurities as the only side product. In this scenario, the effluent from reactor R-3 would contain only butadiene, water, and heavy impurities. The distillation column D-2 in Figure 4 was designed to maximize the recovery of butadiene in the distillate and achieves 99.95 mol% recovery. This distillation column was not used to purify butadiene to the product specification due to the high refrigeration costs associated with

doing so. The distillate, a 97.7 mol% pure butadiene stream with heavy organics as the main impurity, is instead contacted with water in absorption column A-1, yielding a 99.5 mol% pure butadiene stream with only a 0.1% loss of product. The process was simulated with this scenario and the base-case decarbonylation system, and the MSP of butadiene was calculated to be \$4.48 kg<sup>-1</sup>, a  $\sim$ 17% decrease from the base case.

The combined impact of selectivity improvements in reactors R-1 and R-3 was assessed by simulating the process with both of the improved reactor performances. This scenario yielded a butadiene MSP of \$3.80 kg<sup>-1</sup>, a 30% decrease from the base case. This result indicates that the impact of both catalyst improvements together is nearly equal to the sum (30%) of their individual impacts on the butadiene MSP.

Path towards Economic Viability. Although the selectivity improvements in reactors R-1 and R-3 would result in a notable decrease in the MSP of butadiene, the change would still not be sufficient for the process to be profitable under current market conditions. The MSP of butadiene calculated in the hypothetical scenario where both reactors exhibit 95% selectivity at full conversion, \$3.80 kg<sup>-1</sup>, is still 58% higher than the maximum observed butadiene price (\$2.40 kg<sup>-1</sup>) in the last three years. Therefore, the proposed process can only reach economic viability through a combination of technological and economic factors. We considered the cumulative process improvements described above combined with a decrease in the purchase price of furfural; the results are shown in Figure 5. The MSP of butadiene with the hypothetical improved process is only competitive with current prices at a furfural purchase price of \$0.5-1.0 kg<sup>-1</sup>. The base case furfural purchase price for our analysis was \$1.84 kg<sup>-1</sup>, but the market price of furfural briefly reached a minimum of \$0.96 kg<sup>-1</sup> in March 2016. Figure 6 shows the furfural purchase prices considered in Figure 5 (\$1.84 kg<sup>-1</sup>, \$1.50 kg<sup>-1</sup>, \$1.00 kg<sup>-1</sup>, and \$0.50 kg<sup>-1</sup>) with historical prices for comparison. The Chinese market price is used as a proxy for the international market price since 75% of global furfural production takes place in China. This comparison illustrates the potential economic viability of the process in the case of lower furfural prices driven by increased production.

In the above analysis, we have considered a constant base-case butadiene sale price of \$1.1 kg<sup>-1</sup>, but the butadiene market price is also subject to change, as seen in **Figure 5**. **Figure 7** summarizes the combination of economic and technological conditions under which the proposed process would be profitable. The pairs of furfural and butadiene prices which result in a zero net present value lie on the black and red lines, and the shaded regions correspond to combinations of furfural and butadiene prices under which the process is profitable. The gray dashed line shows equal molar costs of furfural and butadiene, corresponding to the break-even prices for a hypothetical process with 100% yield and no processing costs. The hydrogen price is held constant in these calculations since the primary method of hydrogen production (steam reforming) is a mature technology.<sup>78</sup> If furfural supply and butadiene demand continue to grow, or if the manufacture of butadiene from petroleum-derived hydrocarbons becomes more expensive, e.g. due

to a carbon tax, the market prices of furfural and butadiene may shift, improving the economic outlook of the proposed furfural-to-butadiene process.

**Process Sustainability.** The sustainability of the proposed process can be evaluated based on qualitative and quantitative metrics.<sup>79</sup> The most significant design choice from a sustainability standpoint is the use of biomass-derived furfural as a feedstock for butadiene production rather than hydrocarbons. Furfural is typically produced from bagasse or corn cobs,<sup>34</sup> which are renewable, and its production is a way to valorize lignocellulosic biomass. However, the sustainability of biomass-derived furfural depends on the sustainable practices used in the production of those crops.<sup>41</sup> The proposed process also makes use of heat integration to reduce energy consumption; the three process stream heat exchangers reduce the heating and cooling loads each by 3.76 MW, which offsets carbon emissions and water use associated with steam and cooling water.

The construction of a new chemical process has a far-reaching impact on the environment, the economy, and society. Relationally a comprehensive analysis of metrics such as greenhouse gas emissions, water use, and societal impact requires a detailed life-cycle assessment, which is beyond the scope of this work, we evaluate several important quantitative sustainability metrics. The total carbon efficiency of the process is defined as the moles of carbon in the product stream divided by the moles of carbon in the feed stream. With an overall molar yield of 73% from furfural to butadiene, and a loss of 1 mole of CO per mole of furfural, the carbon efficiency of the proposed process is 58.4%. After the CO is oxidized, it exits the process as a stream of CO<sub>2</sub> with a mass flow rate equal to 44.5% of the furfural feed mass flow rate. This stream can be emitted to the environment or captured as a chemical feedstock. Carbon dioxide upgrading remains one of the most widely studied problems in heterogeneous/electro-catalysis, Relational and development of such technologies is anticipated to improve the carbon footprint of the proposed process in the coming decades.

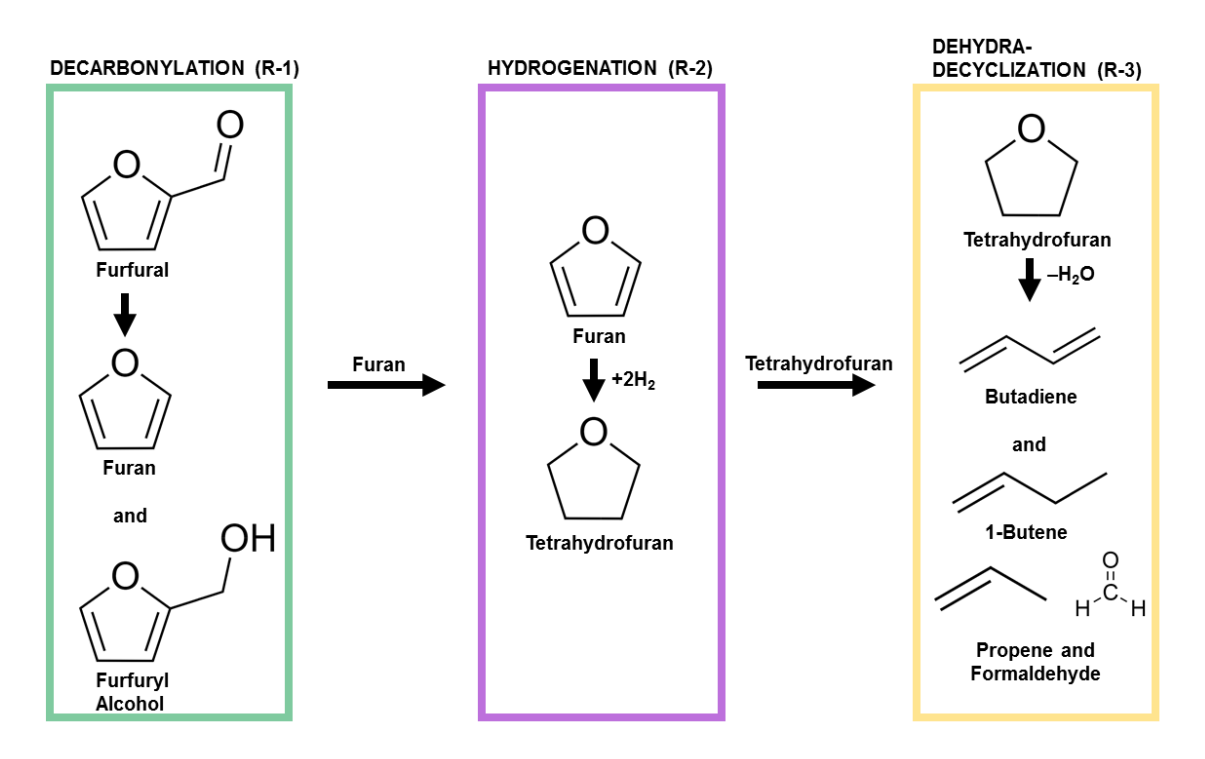
The amount of waste produced by the process can be quantified by the "E factor", defined as the ratio of the total waste mass flow rate to the product mass flow rate.<sup>84</sup> The waste streams in the proposed process are stream 7 (after oxidation, 4273 kg hr<sup>-1</sup>), stream 11 (364 kg hr<sup>-1</sup>), and only the organics in streams 21 and 24 (together, 1410 kg hr<sup>-1</sup>); treated wastewater is excluded from the calculation of the E factor. For a butadiene product flow rate of 3991 kg hr<sup>-1</sup>, this corresponds to an E factor of ~1.5, a typical value for a bulk chemical process.<sup>84</sup> The capture of CO<sub>2</sub> and the use of organic byproducts as fuel could further lower this value.

**4. Conclusions.** The industrial viability of a furfural-to-butadiene synthetic route was investigated through process simulation. The proposed sequence consists of three steps: (i) the decarbonylation of furfural to

furan, (ii) the hydrogenation of furan to tetrahydrofuran (THF), and (iii) the dehydra-decyclization of THF to butadiene. The process was evaluated at a scale of 77 kton yr<sup>-1</sup> (100 kmol hr<sup>-1</sup>) of furfural feed. A discounted cash flow accounting method gave a minimum selling price of butadiene (defined as the price at which the process has a zero net present value) of \$5.43 kg<sup>-1</sup>, well above the current market price of \$1.1 kg<sup>-1</sup>. A sensitivity analysis identified the furfural purchase price as the largest contributor to the cost of the proposed process. An analysis of process parameters isolated the selectivities of the decarbonylation and dehydra-decyclization reactions as the two largest technological opportunities for improving process economics. These improvements were considered alongside economic factors to elucidate the combinations of technological and market conditions which could lead to an improved economic outlook for the process.

**Acknowledgements.** We acknowledge financial support from the National Science Foundation Center for Sustainable Polymers (NSF-CSP) at the University of Minnesota (CHE-1901635) and the Minnesota Corn Growers Association.

**Supporting Information**. The online supporting information includes: process flows and unit operation description, economic evaluation, parameter analysis (rate of return, tax rate, plant size), catalyst cost analysis, and design of auxiliary equipment.



**Scheme 1.** Process chemistry of three sequential reactors to convert furfural to butadiene: furfural decarbonylation (R-1), furan hydrogenation (R-2), and tetrahydrofuran dehydra-decyclization (R-3).

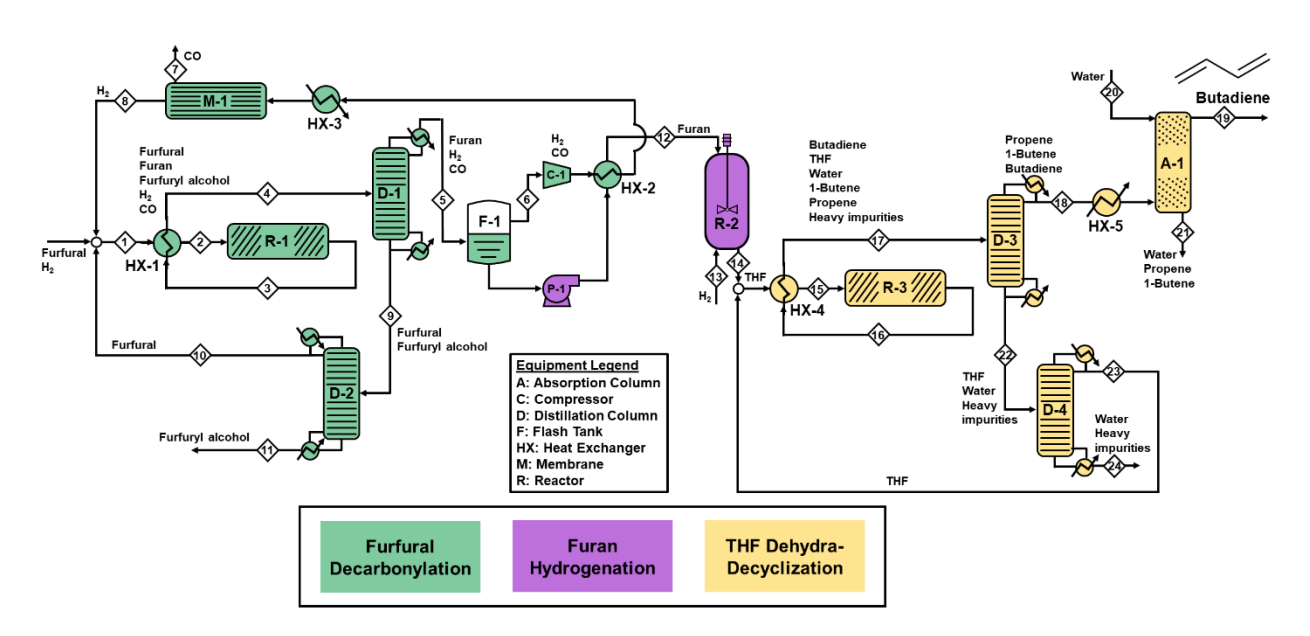


**Figure 1**. Process flow diagram for the conversion of furfural to butadiene via furfural decarbonylation (R-1, D-1, D-2, F-1, C-1, M-1), furan hydrogenation (P-1, R-2), and tetrahydrofuran (THF) dehydradecyclization (R-3, D-3, D-4, A-1).

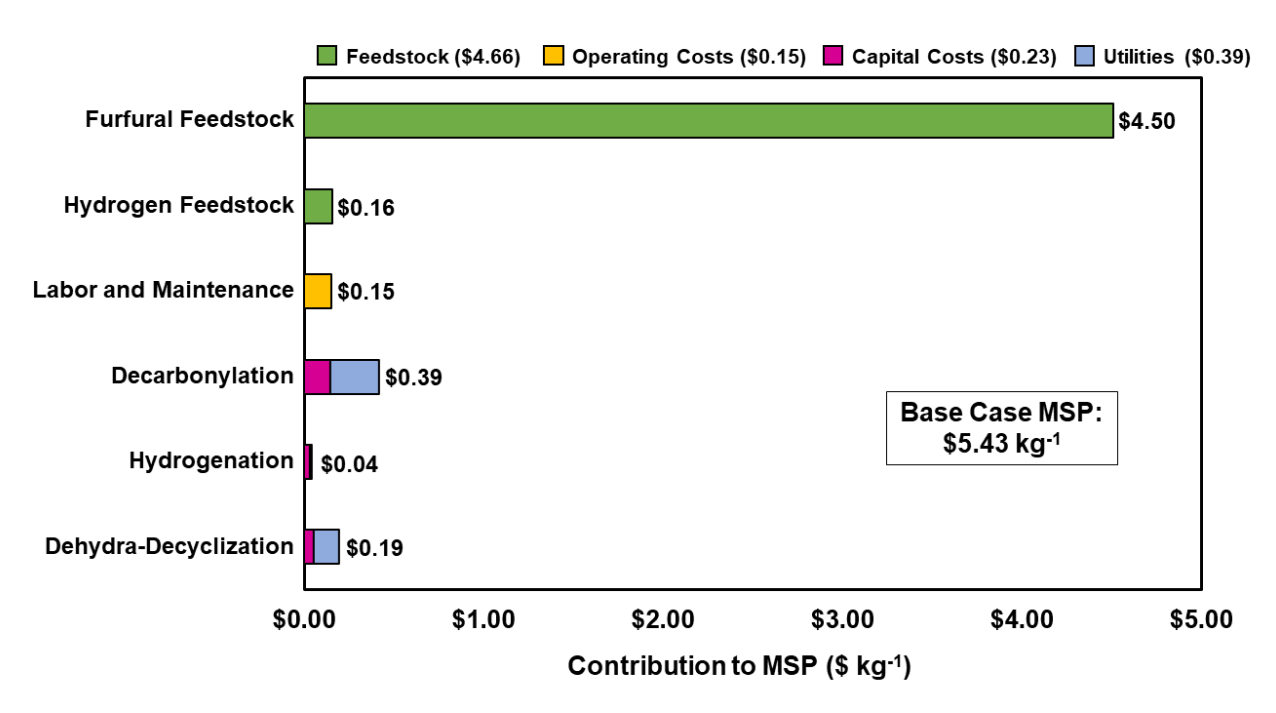
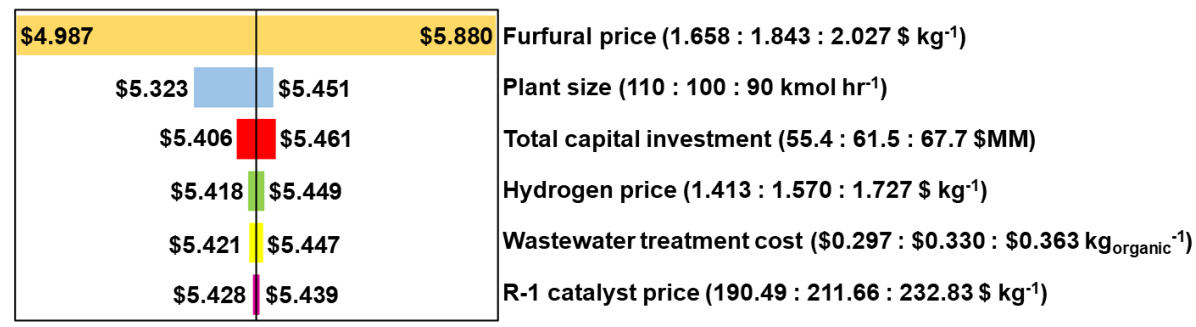


**Figure 2**. Contribution of process costs to the minimum selling price (MSP) of butadiene. Process scale: 77 kton yr<sup>-1</sup> (100 kmol hr<sup>-1</sup>), tax rate: 25%, MARR: 10%, furfural purchase price: \$1.84 kg<sup>-1</sup>.



-\$0.45 -\$0.35 -\$0.25 -\$0.15 -\$0.05 \$0.05 \$0.15 \$0.25 \$0.35 \$0.45

Change in MSP of butadiene (\$ kg<sup>-1</sup>) Base Case: \$5.43 kg<sup>-1</sup>

**Figure 3**. Sensitivity of the minimum selling price (MSP) of butadiene to selected process parameters. Parameters were varied  $\pm 10\%$  relative to the base case design of 100 kmol hr<sup>-1</sup> at furfural and hydrogen purchase prices of \$1.84 kg<sup>-1</sup> and \$1.57 kg<sup>-1</sup> respectively.

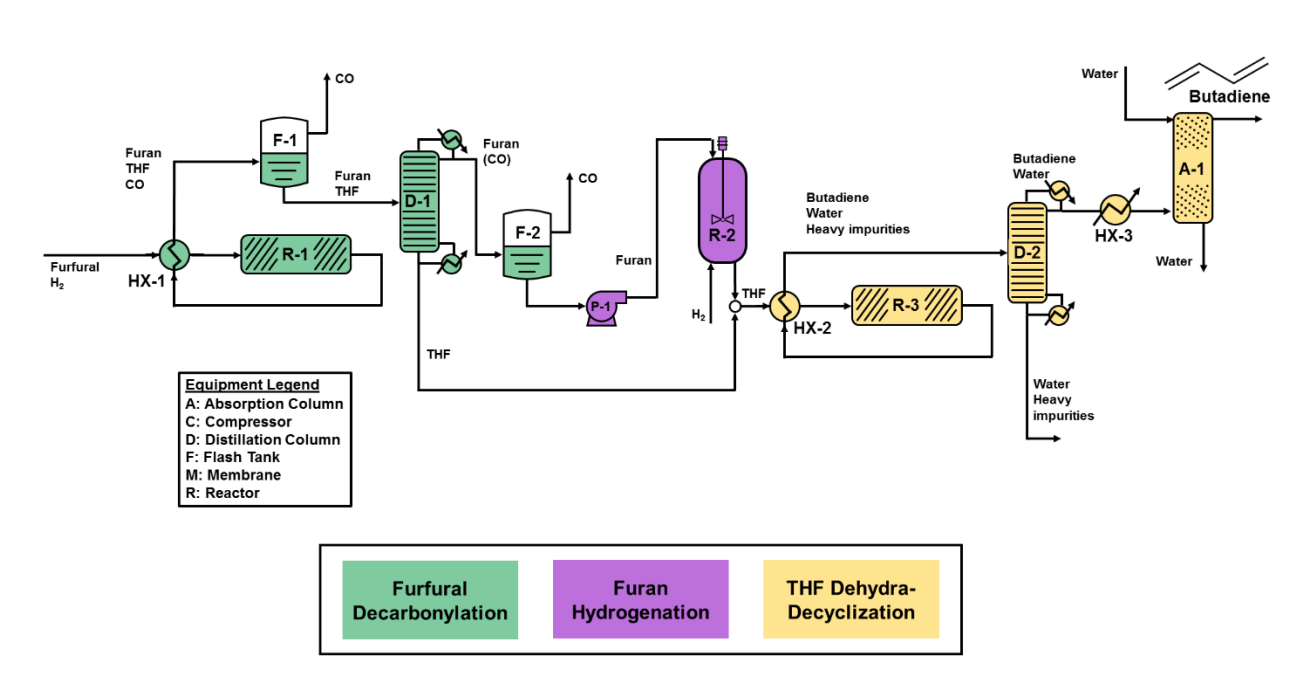


**Figure 4.** Process flow diagram for the furfural-to-butadiene process with hypothetical selectivity improvements in reactors R-1 (furfural decarbonylation) and R-3 (THF dehydra-decyclization). The increased selectivity in each reactor allows for simpler downstream separations. The impact of these improvements on the minimum selling price (MSP) of butadiene is shown in **Figure 5**.

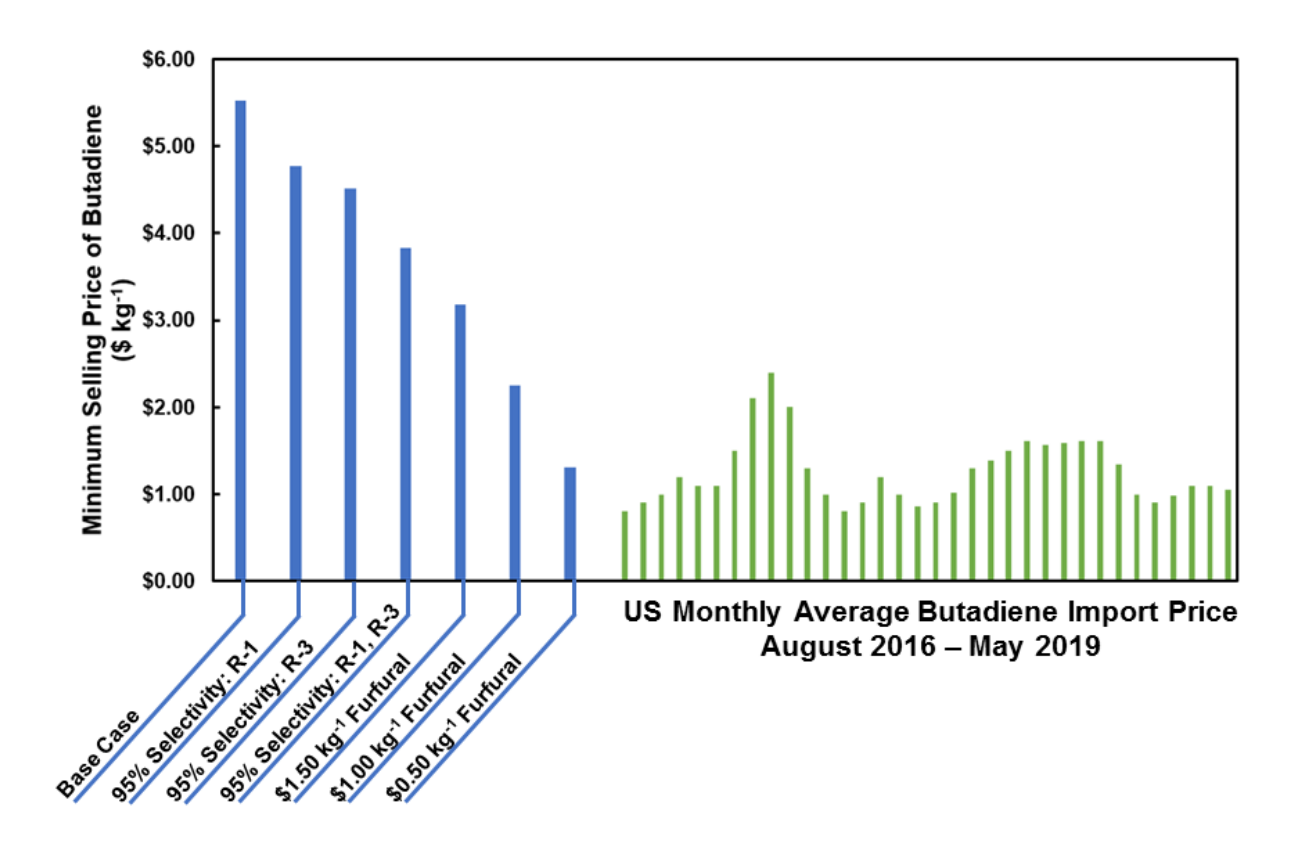


**Figure 5.** Impact of potential selectivity improvements in R-1 (furfural decarbonylation) and R-3 (THF dehydra-decyclization) and furfural feedstock prices on the minimum selling price (MSP) of butadiene. The MSPs for cumulative process improvements are shown in blue. Monthly average import prices for the United States are presented in green for comparison. <sup>76,85,86</sup>

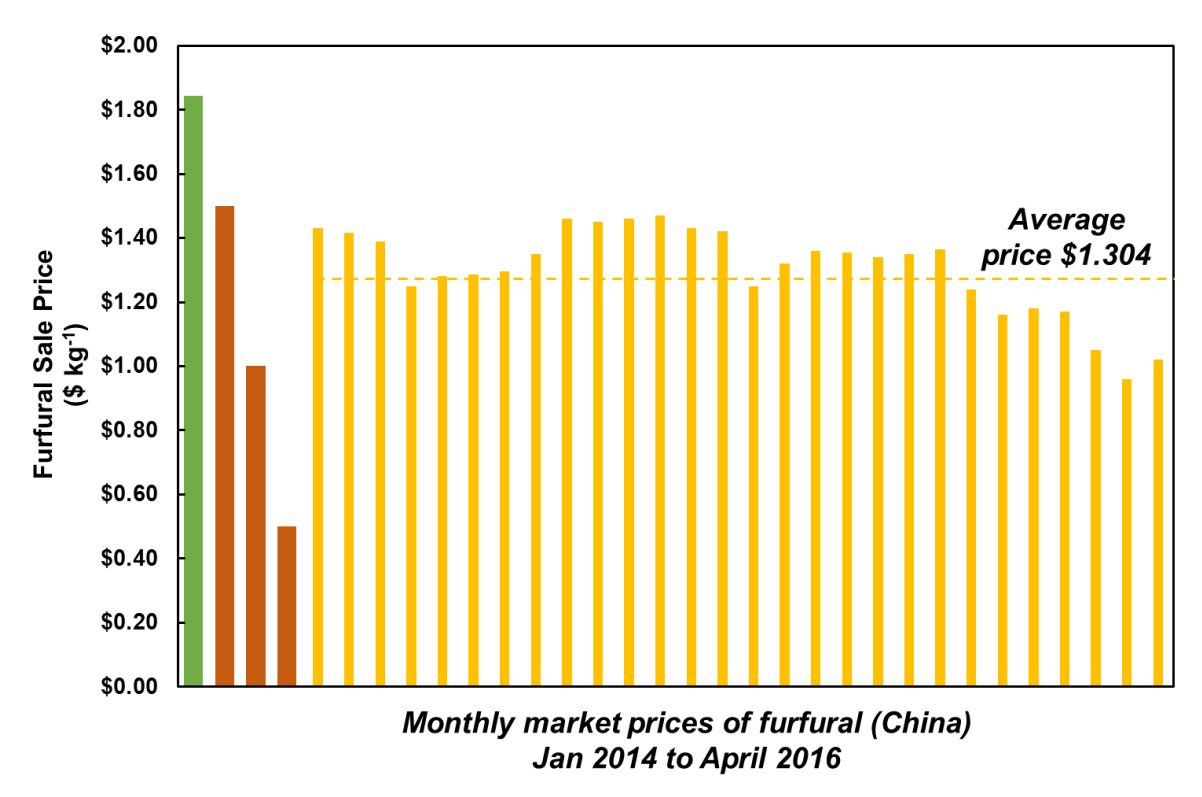


**Figure 6**. Furfural prices<sup>77</sup> considered in **Figure 5** (orange; base case \$1.84 kg<sup>-1</sup> in green) compared to monthly market prices of furfural in China from January 2014 to April 2016 (yellow).<sup>76</sup> Since the Chinese furfural market comprises 75% of the global furfural market, Chinese prices are indicative of international prices.<sup>87,88</sup>

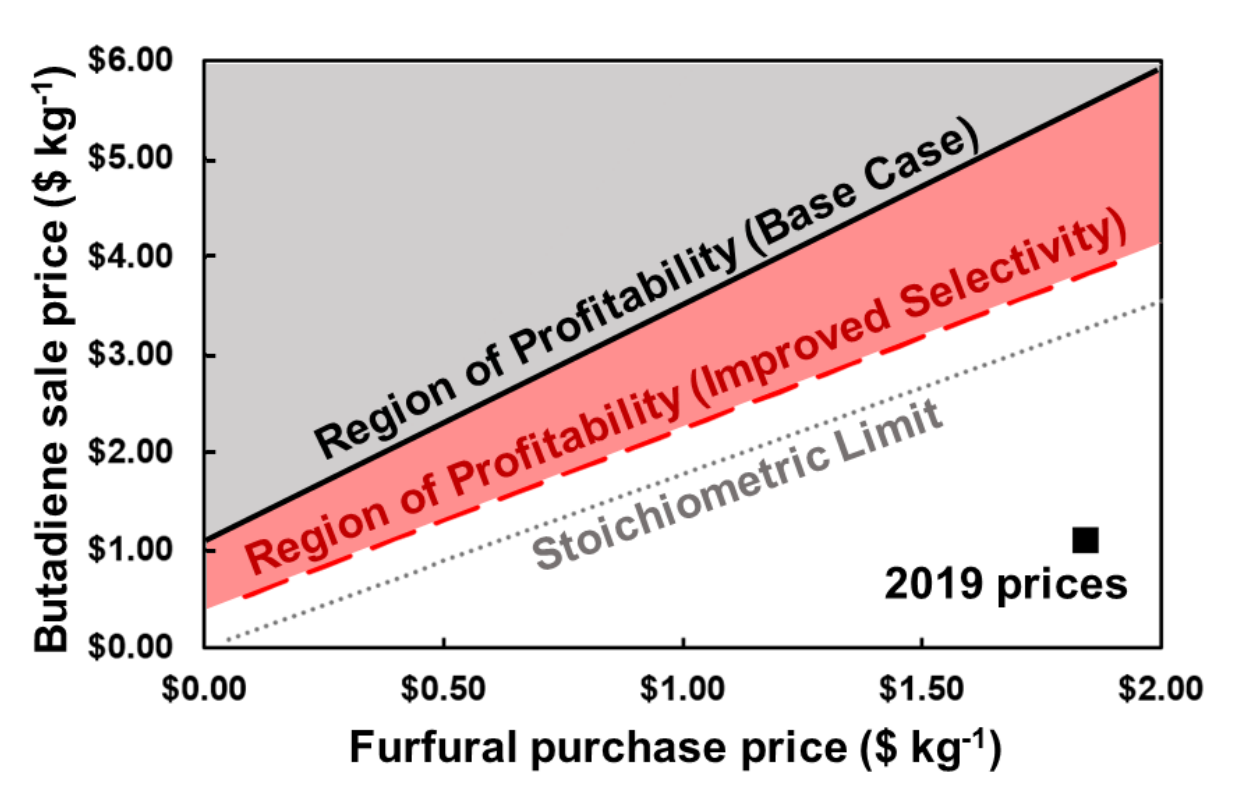


**Figure 7.** The minimum selling price (MSP) of butadiene at varying furfural feedstock prices is shown for the base-case design (black solid line) and the hypothetical design with 95% selectivity in reactors R-1 and R-3 (red dashed line). The gray dashed line corresponds to the minimum profitable butadiene price assuming quantitative conversion and no processing costs. The hydrogen price is held constant at \$1.57 kg<sup>-1</sup>. The base-case prices are shown for comparison. <sup>85,88</sup>

Table 1. Feedstock, Product, and Utility Prices.

Furfural purchase price (\$ kg <sup>-1</sup> ) <sup>88</sup>	1.84
Hydrogen purchase price (\$ kg <sup>-1</sup> ) <sup>89</sup>	1.57
Butadiene sale price (\$ kg <sup>-1</sup> ) 85	1.1
Buttautetic safe price (\$\pi \kg )	1.1
Electricity (\$ kWh <sup>-1</sup> ) a	$7.75 \times 10^{-2}$
Cooling Water (\$ kg <sup>-1</sup> ) <sup>a</sup>	$3.17 \times 10^{-5}$
Refrigerant (\$ kg <sup>-1</sup> ) a	$1.87 \times 10^{-4}$
Steam, 100 psi (\$ kg <sup>-1</sup> ) a	$1.79 \times 10^{-2}$
Natural Gas (\$ SCM <sup>-1</sup> ) <sup>74</sup>	0.213
Wastewater treatment (\$ kg-organic <sup>-1</sup> ) <sup>75</sup>	0.33

<sup>&</sup>lt;sup>a</sup> Estimated in 2013 USD using Aspen Economic Analyzer V8.6, and indexed to 2018 by using Chemical Engineering Plant Cost Index (CEPCI)

Table 2. Process Capital and Operating Costs for the evaluated base case.

<b>Process Section</b>	Capital Cost (\$MM)	Operating Cost (\$MM yr <sup>-1</sup> )
Decarbonylation	39.6	12.0
Hydrogenation	2.2	0.01
Dehydra-Decyclization	15.6	4.7
OSBL <sup>a</sup>	2.9	4.1
Labor and maintenance	<del>-</del>	2.2

<sup>&</sup>lt;sup>a</sup> OSBL (outside battery limits) refers to storage tanks for feedstocks and products as well as a wastewater treatment unit.

### References

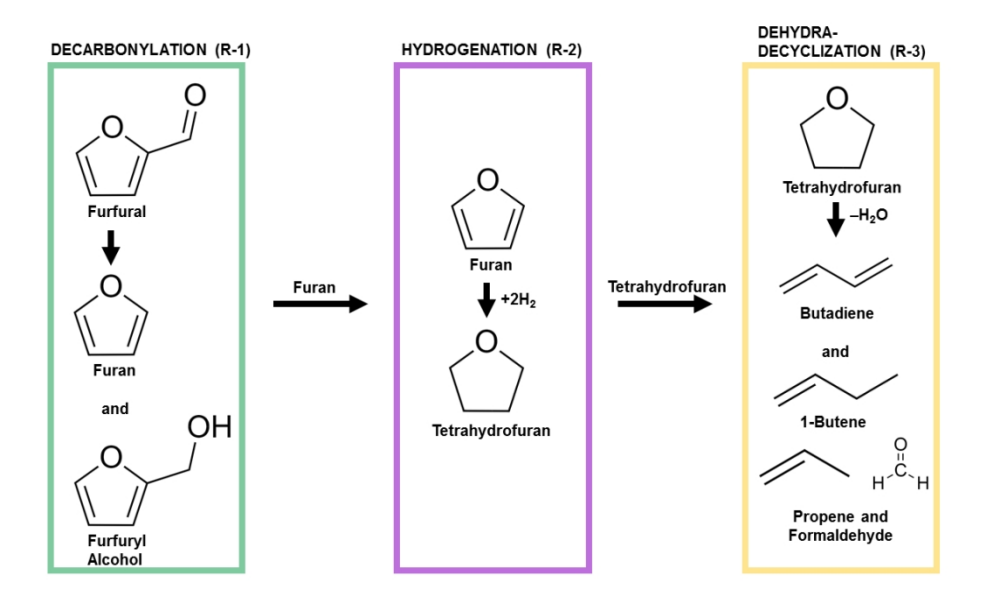
- (1) Zhu, Y.; Romain, C.; Williams, C. K. Sustainable polymers from renewable resources. *Nature* **2016**, *540* (7633), 354–362. DOI: 10.1038/nature21001
- (2) Hillmyer M.A., The promise of plastics from plants. *Science* **2016**, *358* (6365), 868-870. DOI: 10.1126/science.aao6711
- (3) Lundberg, D. J.; Lundberg, D. J.; Hillmyer, M. A.; Dauenhauer, P. J. Techno-economic Analysis of a Chemical Process to Manufacture Methyl- ε -caprolactone from Cresols. ACS Sustain. Chem. Eng. 2018, 6 (11), 15316–15324. DOI: 10.1021/acssuschemeng.8b03774
- (4) Fan, W.; Cho, H. J.; Ren, L.; Vattipailli, V.; Yeh, Y.-H.; Gould, N. G.; Xu, B.; Gorte, R. J.; Lobo, R.; Dauenhauer, P. J.; et al. Renewable p-Xylene from 2,5-Dimethylfuran and Ethylene Using Phosphorus-containing Zeolite Catalysts. *ChemCatChem* **2016**, 9(3), 398-402. DOI: 10.1002/cctc.201601294
- (5) Patet, R. E.; Nikbin, N.; Williams, C. L.; Green, S. K.; Chang, C. C.; Fan, W.; Caratzoulas, S.; Dauenhauer, P. J.; Vlachos, D. G. Kinetic Regime Change in the Tandem Dehydrative Aromatization of Furan Diels-Alder Products. *ACS Catal.* **2015**, *5* (4), 2367–2375. DOI: 10.1021/cs5020783
- (6) Wijaya, Y. P.; Winoto, H. P.; Park, Y. K.; Suh, D. J.; Lee, H.; Ha, J. M.; Jae, J. Heteropolyacid catalysts for Diels-Alder cycloaddition of 2,5-dimethylfuran and ethylene to renewable p-xylene. *Catal. Today* **2017**, *293*–*294*, 167–175. DOI: 10.1016/j.cattod.2016.12.032
- (7) Lundberg, D. J.; Lundberg, D. J.; Zhang, K.; Dauenhauer, P. J. Process Design and Economic Analysis of Renewable Isoprene from Biomass via Mesaconic Acid. *ACS Sustain. Chem. Eng.* **2019**, 7 (5), 5576–5586. DOI: 10.1021/acssuschemeng.9b00362
- (8) Athaley, A.; Annam, P.; Saha, B.; Ierapetritou, M. Techno-economic and life cycle analysis of different types of hydrolysis process for the production of p-Xylene. *Comput. Chem. Eng.* **2019**, *121*, 685–695. DOI: 10.1016/j.compchemeng.2018.11.018
- (9) Olivera, S.; Muralidhara, H. B.; Venkatesh, K.; Gopalakrishna, K.; Vivek, C. S. Plating on acrylonitrile-butadiene-styrene (ABS) plastic: a review. *J. Mater. Sci.* **2016**, *51* (8), 3657–3674 (https://doi.org/10.1007/s10853-015-9668-7).
- (10) Langenthal, W. V; Schnetger, J. *Processing of Natural and Synthetic Rubber*; Wiley-VCH, 2005 (https://doi.org/10.1002/3527600035.bpol2008).
- (11) Furukawa, S.; Endo, M.; Komatsu, T. Bifunctional catalytic system effective for oxidative dehydrogenation of 1-butene and n -butane using Pd-based intermetallic compounds. *ACS Catal.* **2014**, *4* (10), 3533–3542. DOI: 10.1021/cs500920p
- (12) Cespi, D.; Passarini, F.; Vassura, I.; Cavani, F. Butadiene from biomass, a life cycle perspective to address sustainability in the chemical industry. *Green Chem.* **2016**, *18* (6), 1625–1638. DOI: 10.1039/c5gc02148k
- (13) Bruijnincx, P. C. A.; Weckhuysen, B. M. Shale gas revolution: An opportunity for the production of biobased chemicals? *Angew. Chemie Int. Ed.* **2013**, *52* (46), 11980–11987. DOI: 10.1002/anie.201305058
- (14) Makshina, E. V.; Dusselier, M.; Janssens, W.; Degrève, J.; Jacobs, P. A.; Sels, B. F. Review of old chemistry and new catalytic advances in the on-purpose synthesis of butadiene. *Chem. Soc. Rev.* **2014**, *43* (22), 7917–7953. DOI: 10.1039/c4cs00105b
- (15) Abdelrahman, O. A.; Park, D. S.; Vinter, K. P.; Spanjers, C. S.; Ren, L.; Cho, H. J.; Vlachos, D. G.; Fan, W.; Tsapatsis, M.; Dauenhauer, P. J. Biomass-Derived Butadiene by Dehydra-Decyclization of Tetrahydrofuran. *ACS Sustain. Chem. Eng.* **2017**, 5(5), 3732-3736. DOI: 10.1021/acssuschemeng.7b00745.
- (16) Ho, C. R.; Shylesh, S.; Bell, A. T. Mechanism and Kinetics of Ethanol Coupling to Butanol over Hydroxyapatite. *ACS Catal.* **2016**, *6* (2), 939–948 (https://doi.org/10.1021/acscatal.5b02672).
- (17) Ipatieff, V. To the question of the decomposition of ethyl alcohol due to various catalysts. *J. Russ. Phys. Chem. Soc.* **1903**, *35*, 449–452.

- (18) S. V. Lebedev, British Pat. 331, 402, 1929.
- (19) Kyriienko, P. I.; Larina, O. V.; Soloviev, S. O.; Orlyk, S. M.; Calers, C.; Dzwigaj, S. Ethanol Conversion into 1,3-Butadiene by the Lebedev Method over MTaSiBEA Zeolites (M = Ag, Cu, Zn). *ACS Sustain. Chem. Eng.* **2017**, *5* (3), 2075–2083 (https://doi.org/10.1021/acssuschemeng.6b01728).
- (20) Sato, S.; Sato, F.; Gotoh, H.; Yamada, Y. Selective dehydration of alkanediols into unsaturated alcohols over rare earth oxide catalysts. *ACS Catal.* **2013**, *3* (4), 721–734 (https://doi.org/10.1021/cs300781v).
- (21) Fang, L.; Jing, F.; Lu, J.; Hu, B.; Pera-Titus, M. Nano-flowered Ce@MOR hybrids with modulated acid properties for the vapor-phase dehydration of 1,3-butanediol into butadiene. *Green Chem.* **2017**, *19* (19), 4610–4621 (https://doi.org/10.1039/C7GC02223A).
- (22) Zeng, F.; Tenn, W. J.; Aki, S. N. V. K.; Xu, J.; Liu, B.; Hohn, K. L. Influence of basicity on 1,3-butadiene formation from catalytic 2,3-butanediol dehydration over γ-alumina. *J. Catal.* 2016, 344, 77–89 (https://doi.org/10.1016/j.jcat.2016.09.003).
- (23) Lanzafame, P.; Centi, G.; Perathoner, S. Catalysis for biomass and CO2use through solar energy: Opening new scenarios for a sustainable and low-carbon chemical production. *Chem. Soc. Rev.* **2014**, *43* (22), 7562–7580 (https://doi.org/10.1039/C3CS60396B).
- Ji, X. J.; Huang, H.; Ouyang, P. K. Microbial 2,3-butanediol production: A state-of-the-art review. *Biotechnol. Adv.* **2011**, *29* (3), 351–364 (https://doi.org/10.1016/j.biotechadv.2011.01.007).
- (25) Liu, X.; Fabos, V.; Taylor, S.; Knight, D. W.; Whiston, K.; Hutchings, G. J. One-Step Production of 1,3-Butadiene from 2,3-Butanediol Dehydration. *Chem. A Eur. J.* **2016**, *22* (35), 12290–12294.
- (26) Vecchini, N; Galeotti, A; Pisano, A; Process for the production of 1,3-butadiene from 1,4 butaneidol via tetrahydrofuran. *International patent number WO 2016/092517 A1*, 2016 (https://doi.org/10.1002/chem.201602390).
- (27) Yim, H.; Haselbeck, R.; Niu, W.; Pujol-Baxley, C.; Burgard, A.; Boldt, J.; Khandurina, J.; Trawick, J. D.; Osterhout, R. E.; Stephen, R.; et al. Metabolic engineering of Escherichia coli for direct production of 1,4-butanediol. *Nat. Chem. Biol.* **2011**, *7* (7), 445–452 (https://doi.org/10.1038/nchembio.580).
- (28) Chheda, J. N.; Román-Leshkov, Y.; Dumesic, J. A. Production of 5-hydroxymethylfurfural and furfural by dehydration of biomass-derived mono- and poly-saccharides. *Green Chem.* **2007**, *9* (4), 342–350 (https://doi.org/10.1039/B611568C).
- (29) Song, D.; Yoon, Y. G.; Lee, C. J. Conceptual design for the recovery of 1,3-Butadiene and methyl ethyl ketone via a 2,3-Butanediol-dehydration process. *Chem. Eng. Res. Des.* **2017**, *123*, 268–276 (https://doi.org/10.1016/j.cherd.2017.05.019).
- (30) Song, D.; Yoon, Y. G.; Lee, C. J. Techno-economic evaluation of the 2,3-butanediol dehydration process using a hydroxyapatite-alumina catalyst. *Korean J. Chem. Eng.* **2018**, *35* (12), 2348–2354 (https://doi.org/10.1007/s11814-018-0161-2).
- (31) Chambers, J. M. Extractive distillation. World Pet. Congr. Proc. 1951, 1951-May, 90–106.
- (32) Athaley, A.; Saha, B.; Ierapetritou, M. Biomass-based chemical production using techno-economic and life cycle analysis. *AIChE J.* **2019**, *65* (9) (https://doi.org/10.1002/aic.16660).
- Outta, S.; De, S.; Saha, B.; Alam, M. I. Advances in conversion of hemicellulosic biomass to furfural and upgrading to biofuels. *Catal. Sci. Technol.* **2012**, *2* (10), 2025–2036 (https://doi.org/10.1039/C2CY20235B).
- (34) Cai, C. M.; Zhang, T.; Kumar, R.; Wyman, C. E. Integrated furfural production as a renewable fuel and chemical platform from lignocellulosic biomass. *J. Chem. Technol. Biotechnol.* **2014**, *89* (1), 2–10 (https://doi.org/10.1002/jctb.4168).
- (35) Mettler, M. S.; Paulsen, A. D.; Vlachos, D. G.; Dauenhauer, P. J. Tuning cellulose pyrolysis chemistry: Selective decarbonylation via catalyst-impregnated pyrolysis. *Catal. Sci. Technol.* **2014**, *4* (11), 3822–3825 (https://doi.org/10.1039/C4CY00676C).
- (36) Mettler, M. S.; Mushrif, S. H.; Paulsen, A. D.; Javadekar, A. D.; Vlachos, D. G.; Dauenhauer, P. J. Revealing pyrolysis chemistry for biofuels production: Conversion of cellulose to furans and small

- oxygenates. Energy Environ. Sci. 2012, 5 (1), 5414–5424 (DOI: 10.1039/C1EE02743C).
- (37) Biddy, M. J.; Scarlata, C.; Kinchin, C. Chemicals from Biomass: A Market Assessment of Bioproducts with Near-Term Potential. **2016**, NREL Technical report (NREL/TP-5100-65509) (available at www.nrel.gov/publications). Retreived: Dec. 15, 2020.
- (38) Gürbüz, E. I.; Wettstein, S. G.; Dumesic, J. A. Conversion of hemicellulose to furfural and levulinic acid using biphasic reactors with alkylphenol solvents. *ChemSusChem* **2012**, *5* (2), 383–387 (https://doi.org/10.1002/cssc.201100608).
- (39) Alonso, D. M.; Wettstein, S. G.; Mellmer, M. A.; Gurbuz, E. I.; Dumesic, J. A. Integrated conversion of hemicellulose and cellulose from lignocellulosic biomass. *Energy Environ. Sci.* **2013**, *6* (1), 76–80 (https://doi.org/10.1039/C2EE23617F).
- (40) Engler, R. E. Green Chemistry. *Encycl. Toxicol.* **2005**, No. 207890, 471–472.
- (41) Paulino-Flores, M.; Martínez-Campos, Á. R.; Martínez-Castañeda, F. E.; López-Orona, C. A.; Vizcarra-Bordi, I.; Munguía, N. Evaluation of the sustainability of hybrid and native maize production systems. *J. Clean. Prod.* **2017**, *150*, 287–293 (https://doi.org/10.1016/j.jclepro.2017.02.182).
- (42) Bozell, J. J.; Petersen, G. R. Technology development for the production of biobased products from biorefinery carbohydrates—the US Department of Energy's "Top 10" revisited. *Green Chem.* **2010**, *12* (4), 539 (https://doi.org/10.1039/B922014C).
- (43) Furfural Market Expected to Reach \$1,434 Million, Globally by 2022 https://www.alliedmarketresearch.com/press-release/furfural-market.html (accessed 10/13/19)
- Furfural: A renewable and versatile platform molecule for the synthesis of chemicals and fuels. *Energy Environ. Sci.* **2016**, *9* (4), 1144–1189 (https://doi.org/10.1039/C5EE02666K).
- (45) Bhogeswararao, S.; Srinivas, D. Catalytic conversion of furfural to industrial chemicals over supported Pt and Pd catalysts. *J. Catal.* **2015**, *327*, 65–77 (DOI: 10.1016/j.jcat.2015.04.018)
- (46) Sitthisa, S.; An, W.; Resasco, D. E. Selective conversion of furfural to methylfuran over silicasupported NiFe bimetallic catalysts. *J. Catal.* **2011**, *284* (1), 90–101 (https://doi.org/10.1016/j.jcat.2015.04.018).
- (47) Lee, J.; Kr, D.; Chan, H.; Kr, J.; Koh, J. S. US9,527,826 B2. **2016**.
- (48) Sitthisa, S.; Resasco, D. E. Hydrodeoxygenation of furfural over supported metal catalysts: A comparative study of Cu, Pd and Ni. *Catal. Letters* **2011**, *141* (6), 784–791 (https://doi.org/10.1007/s10562-011-0581-7).
- (49) García-Suárez, E. J.; Balu, A. M.; Tristany, M.; García, A. B.; Philippot, K.; Luque, R. Versatile dual hydrogenation-oxidation nanocatalysts for the aqueous transformation of biomass-derived platform molecules. *Green Chem.* **2012**, *14* (5), 1434–1439 (https://doi.org/10.1039/C2GC35176E).
- (50) Sitthisa, S.; Pham, T.; Prasomsri, T.; Sooknoi, T.; Mallinson, R. G.; Resasco, D. E. Conversion of furfural and 2-methylpentanal on Pd/SiO2 and Pd-Cu/SiO2 catalysts. *J. Catal.* **2011**, *280* (1), 17–27 (https://doi.org/10.1016/j.jcat.2011.02.006).
- Zhang, W.; Zhu, Y.; Niu, S.; Li, Y. A study of furfural decarbonylation on K-doped Pd/Al2O 3 catalysts. *J. Mol. Catal. A Chem.* **2011**, *335* (1–2), 71–81 (https://doi.org/10.1016/j.molcata.2010.11.016).
- Jung, K. J.; Gaset, A.; Molinier, J. Furfural decarbonylation catalyzed by charcoal supported palladium: Part II A continuous process. *Biomass* **1988**, *16*, 89–96 (https://doi.org/10.1016/0144-4565(88)90018-2).
- (53) Li K, Ozer R, United States Patent 8,404,871 B2. **2013**.
- (54) Wambach, L.; Irgang, M.; Fischer, M.; Raymond, P. E. L. United States Patent 4,780,552. 1988.
- Pushkarev, V. V.; Musselwhite, N.; An, K.; Alayoglu, S.; Somorjai, G. A. High structure sensitivity of vapor-phase furfural decarbonylation/ hydrogenation reaction network as a function of size and shape of Pt nanoparticles. *Nano Lett.* **2012**, *12* (10), 5196–5201 (https://doi.org/10.1021/nl3023127).
- (56) An, K.; Musselwhite, N.; Kennedy, G.; Pushkarev, V. V.; Robert Baker, L.; Somorjai, G. A. Preparation of mesoporous oxides and their support effects on Pt nanoparticle catalysts in catalytic

- hydrogenation of furfural. *J. Colloid Interface Sci.* **2013**, *392* (1), 122–128 (https://doi.org/10.1016/j.jcis.2012.10.029).
- (57) Smith H.A.; Fuzek, J. F. Catalytic Hydrogenation of Furan and Substituted Furans on Platinum. *J Am. Chem. Soc.* **1949**, *71* (2), 415-419 (https://doi.org/10.1021/ja01170a013).
- (58) Mironenko, A. V.; Gilkey, M. J.; Panagiotopoulou, P.; Facas, G.; Vlachos, D. G.; Xu, B. Ring activation of furanic compounds on ruthenium-based catalysts. *J. Phys. Chem. C* **2015**, *119* (11), 6075–6085 (https://doi.org/10.1021/jp512649b).
- (59) Godawa, C.; Rigal, L.; Gaset, A. Palladium catalyzed hydrogenation of furan: optimization of production conditions for tetrahydrofuran. *Resour. Conserv. Recycl.* **1990**, *3* (4), 201–216 (https://doi.org/10.1016/0921-3449(90)90018-Y).
- (60) Heisig, G. B. 1,4-Diiodobutane from Tetrahydrofuran. *J. Am. Chem. Soc.* **1939** 61 (2), 525-526 (https://doi.org/10.1021/ja01871a507).
- (61) Banford, W. H., Lewiston, N. Y., and Manes, M. M. United States Patent 2,846,449. 1958.
- (62) Li S, Abdelrahman O.A., Kumar G., Tsapatsis M, Vlachos D, Caratzoulas S, Dauenhauer P.J.. Dehydra-Decyclization of Tetrahydrofuran on H-ZSM5: Mechanisms, Pathways, and Role of Transition State Entropy, *ACS Catalysis* **2019**, 9, 10279-10293 (https://doi.org/10.1021/acscatal.9b03129).
- (63) Abdelrahman, O. A.; Park, D. S.; Vinter, K. P.; Spanjers, C. S.; Ren, L.; Cho, H. J.; Vlachos, D. G.; Fan, W.; Tsapatsis, M.; Dauenhauer, P. J. Biomass-Derived Butadiene by Dehydra-Decyclization of Tetrahydrofuran. *ACS Sustain. Chem. Eng.* **2017**, *5* (5), 3732–3736 (https://doi.org/10.1021/acssuschemeng.7b00745).
- (64) Chemical Engineering Plant Cost Index: 2018 Annual Value [online] (https://www.chemengonline.com/2019-cepci-updates-january-prelim-and-december-2018-final/) (accessed 10/13/19).
- (65) Argyle, M.; Bartholomew, C. Heterogeneous Catalyst Deactivation and Regeneration: A Review. *Catalysts* **2015**, *5* (1), 145–269 (https://doi.org/10.3390/catal5010145).
- (66) DiMartino, S. P.; Glazer, J. L.; Houston, C. D.; Schott, M. E. Hydrogen/carbon monoxide separation with cellulose acetate membranes. *Gas Sep. Purif.* **1988**, *2* (3), 120–125 (https://doi.org/10.1016/0950-4214(88)80027-6).
- (67) Oliver F Campbell, William H Decker United States Patent US2753925A, 1951.
- (68) Kantarci, N.; Borak, F.; Ulgen, K. O. Bubble column reactors. *Process Biochem.* **2005**, *40* (7), 2263–2283 (doi:10.1016/j.procbio.2004.10.004).
- (69) Abdelrahman, O. A.; Park, D. S.; Vinter, K. P.; Spanjers, C. S.; Ren, L.; Cho, H. J.; Zhang, K.; Fan, W.; Tsapatsis, M.; Dauenhauer, P. J. Renewable Isoprene by Sequential Hydrogenation of Itaconic Acid and Dehydra-Decyclization of 3-Methyl-Tetrahydrofuran. *ACS Catal.* **2017**, *7* (2), 1428–1431 (https://doi.org/10.1021/acscatal.6b03335).
- (70) Reed, C. D.; Mcketta, J. J. Solubility of 1,3-Butadiene in Water. *J. Chem. Eng. Data* **1959**, *4* (4), 294–295 (https://doi.org/10.1021/je60004a002).
- (71) Serra, M. C. C.; Mainar, A. M.; Palavra, A. M. F. Solubility of ethene in water and in a medium for the cultivation of a bacterial strain. *J. Chem. Eng. Data* **2011**, *56* (4), 1596–1601 (https://doi.org/10.1021/je101248q).
- (72) Azarnoosh, A.; Mcketta, J. J. Solubility of Propylene in Water Apparatus . *J. Chem. Engg. data*, **1959**, *4* (3), 211-212 (https://doi.org/10.1021/je60003a006).
- (73) Golden, G.; Mann, R. H. Isoprene in Kirk, 2nd ed.; Wiley-VCH: New York, 2000.
- (74) https://energies.airliquide.com/resources-planet-hydrogen/how-hydrogen-stored (accessed 10/13/19).
- (75) Warren D. Seider, Daniel R. Lewin, J. D. Seader, Soemantri Widagdo, Rafiqul Gani, K. M. N. *Product and Process Design Principles: Synthesis, Analysis and Evaluation*, 4th ed.; Wiley-VCH, 2016 (ISBN: 978-1-119-28263-1).
- (76) https://www.icis.com/explore/resources/news/2018/11/01/10276397/global-pressure-pulls-down-us-butadiene/ (accessed 10/13/19).

- (77) http://www.cnchemicals.com/Press/86385-CCM: Chinas market price of furfural bounces back in April.html (accessed 10/13/19).
- (78) Mueller-Langer, F.; Tzimas, E.; Kaltschmitt, M.; Peteves, S. Techno-economic assessment of hydrogen production processes for the hydrogen economy for the short and medium term. *Int. J. Hydrogen Energy* **2007**, *32* (16), 3797–3810 (https://doi.org/10.1016/j.ijhydene.2007.05.027).
- (79) Allen, D.T.; Hwang, B-J; Licence, P.; Pradeep, T., Subramaniam B. Advancing the use of sustainability metrics. *ACS Sustain. Chem. Eng.* **2015**, *3* (10), 2359–2360 (https://doi.org/10.1021/acssuschemeng.5b01026).
- (80) Giraud, R. J.; Williams, P. A.; Sehgal, A.; Ponnusamy, E.; Phillips, A. K.; Manley, J. B. Implementing green chemistry in chemical manufacturing: A survey report. *ACS Sustain. Chem. Eng.* **2014**, *2* (10), 2237–2242 (https://doi.org/10.1021/sc500427d).
- (81) Russell, D. A. M.; Shiang, D. L. Thinking about more sustainable products: Using an efficient tool for sustainability education, innovation, and project management to encourage sustainability thinking in a multinational corporation. *ACS Sustain. Chem. Eng.* **2013**, *I* (1), 2–7 (https://doi.org/10.1021/sc300131e).
- (82) Aresta, M.; Dibenedetto, A.; Angelini, A. Catalysis for the valorization of exhaust carbon: From CO2 to chemicals, materials, and fuels. technological use of CO2. *Chem. Rev.* **2014**, *114* (3), 1709–1742 (https://doi.org/10.1021/cr4002758).
- (83) Ginsoke, G. Change is in the air. *Automot. Eng.* **2000**, *25* (2), 82–85.
- (84) Sheldon, R. A. The e Factor: Fifteen years on. *Green Chem.* **2007**, *9* (12), 1273–1283 https://doi.org/10.1039/B713736M).
- (85) https://www.icis.com/explore/commodities/chemicals/butadiene-c4s/ (accessed 10/13/19).
- (86) https://www.argusmedia.com/en/petrochemicals/argus-c-5-and-hydrocarbon-resins-services (accessed 10/13/19).
- (87) Olcay, H.; Malina, R.; Upadhye, A. A.; Hileman, J. I.; Huber, G. W.; Barrett, S. R. H. Technoeconomic and environmental evaluation of producing chemicals and drop-in aviation biofuels via aqueous phase processing. *Energy Environ. Sci.* **2018**, *11* (8), 2085–2101 (https://doi.org/10.1039/C7EE03557H).
- (88) http://www.cnchemicals.com/Detail/Readonline.aspx?id=8180&type=n&cid=20879696885 (accessed 10/13/19).
- (89) Davis, R.; Tao, L.; Scarlata, C.; Tan, E. C. D.; Ross, J.; Lukas, J.; Sexton, D. *Process Design and Economics for the Conversion of Lignocellulosic Biomass to Hydrocarbons: Dilute-Acid and Enzymatic Deconstruction of Biomass to Sugars and Catalytic Conversion of Sugars to Hydrocarbons*; United States: N. p., 2015. Web. doi:10.2172/1176746.



Scheme 1 338x190mm (96 x 96 DPI)

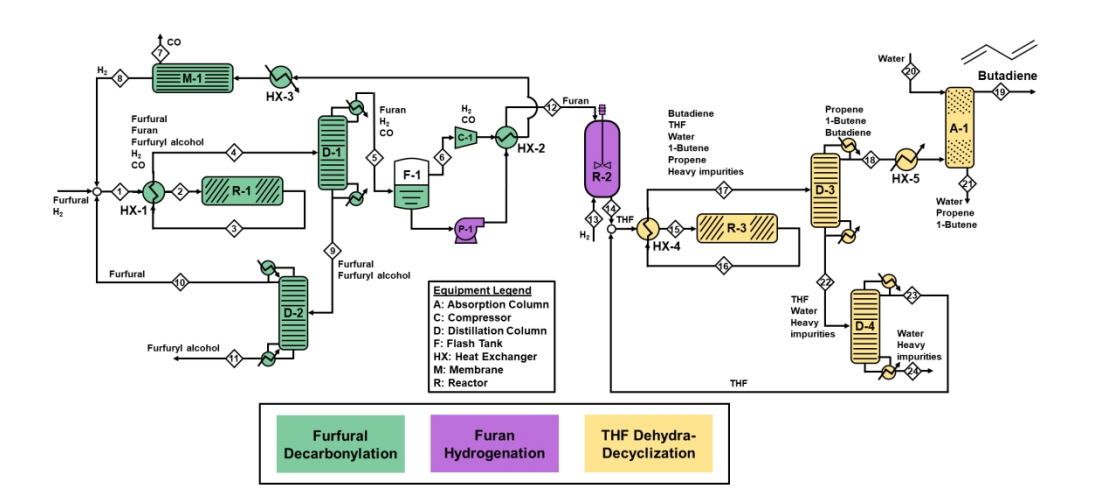


Figure 1
584x279mm (96 x 96 DPI)

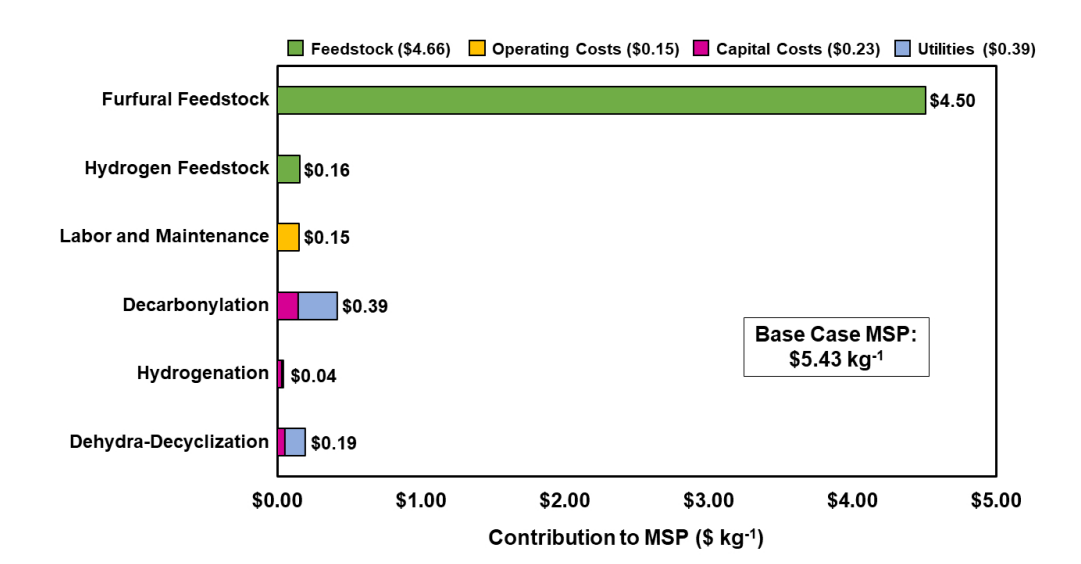


Figure 2
338x190mm (96 x 96 DPI)



-\$0.45 -\$0.35 -\$0.25 -\$0.15 -\$0.05 \$0.05 \$0.15 \$0.25 \$0.35 \$0.45 Change in MSP of butadiene (\$ kg<sup>-1</sup>) Base Case: \$5.43 kg<sup>-1</sup>

Figure 3 389x134mm (96 x 96 DPI)

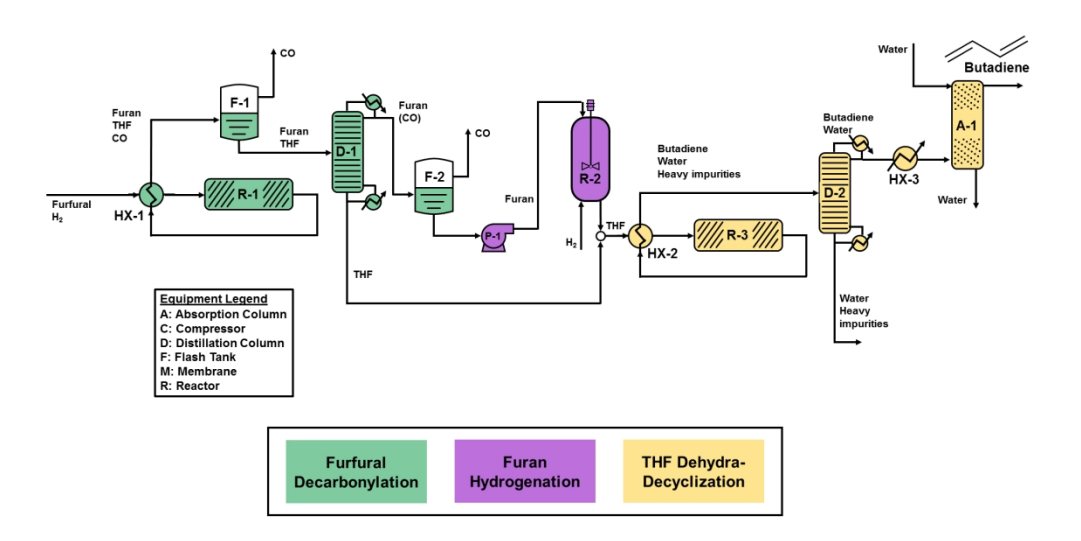


Figure 4
533x279mm (96 x 96 DPI)

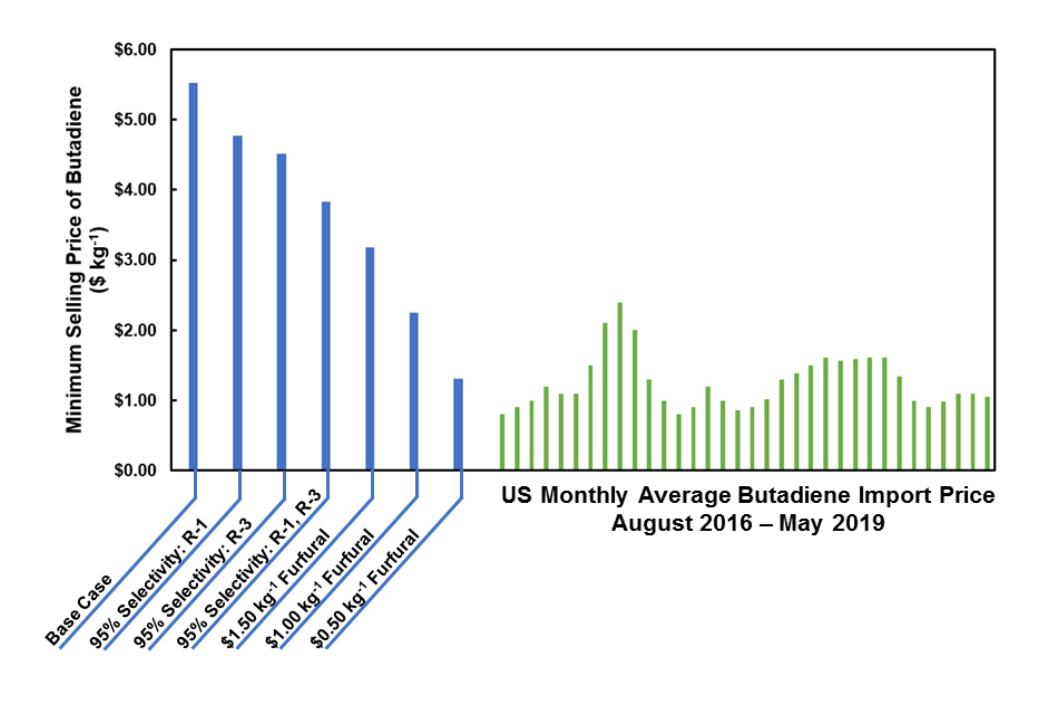


Figure 5
237x165mm (96 x 96 DPI)

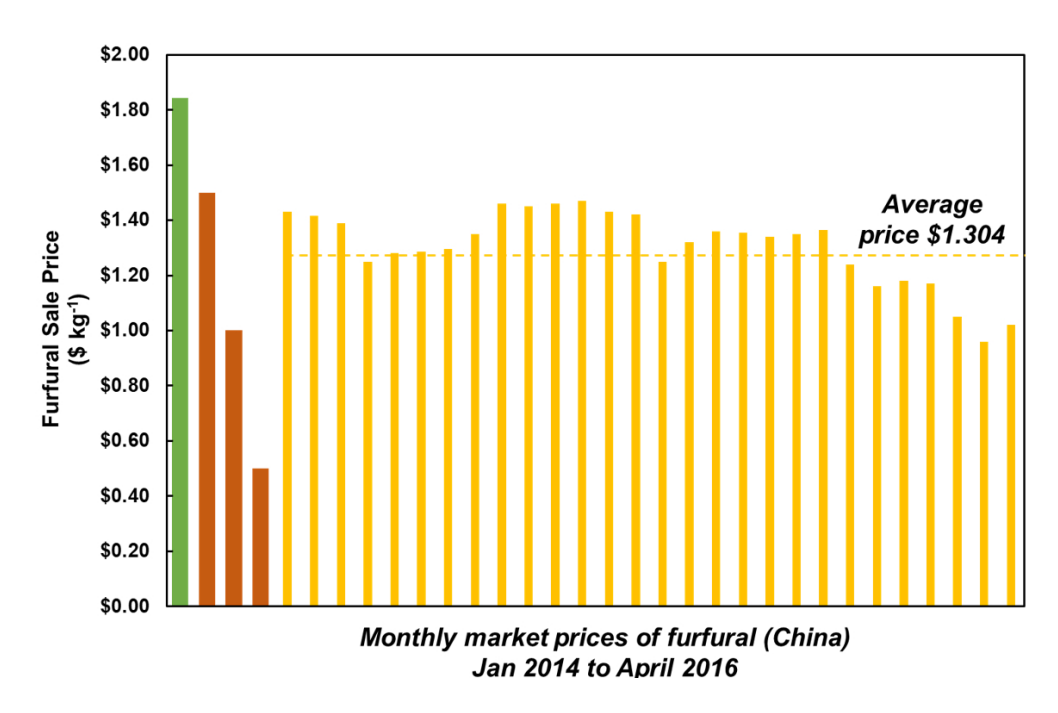


Figure 6 245x155mm (120 x 120 DPI)

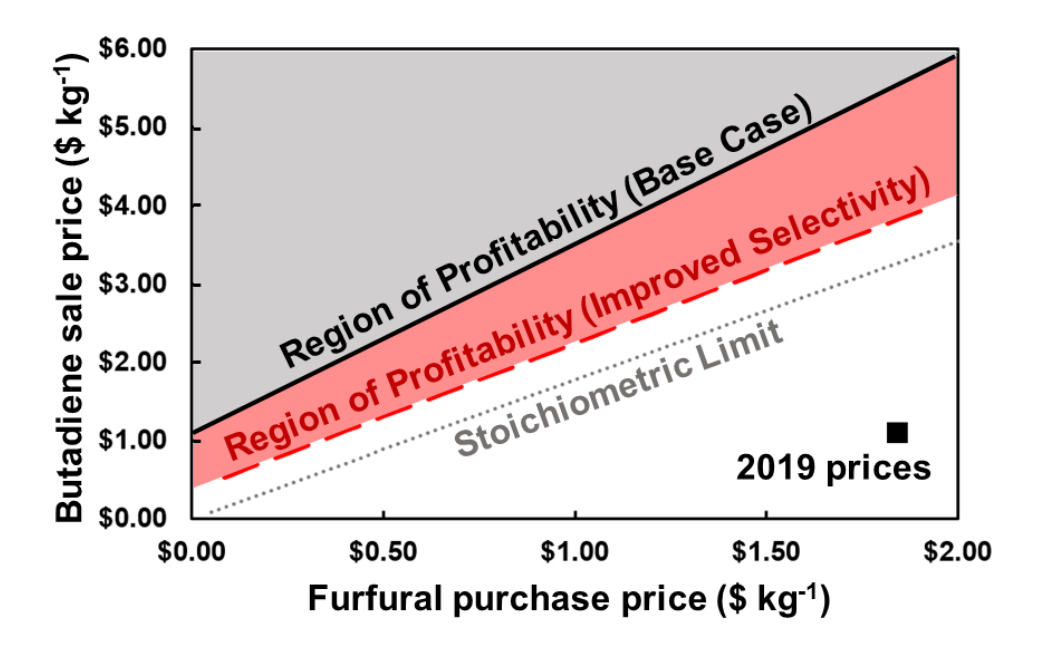
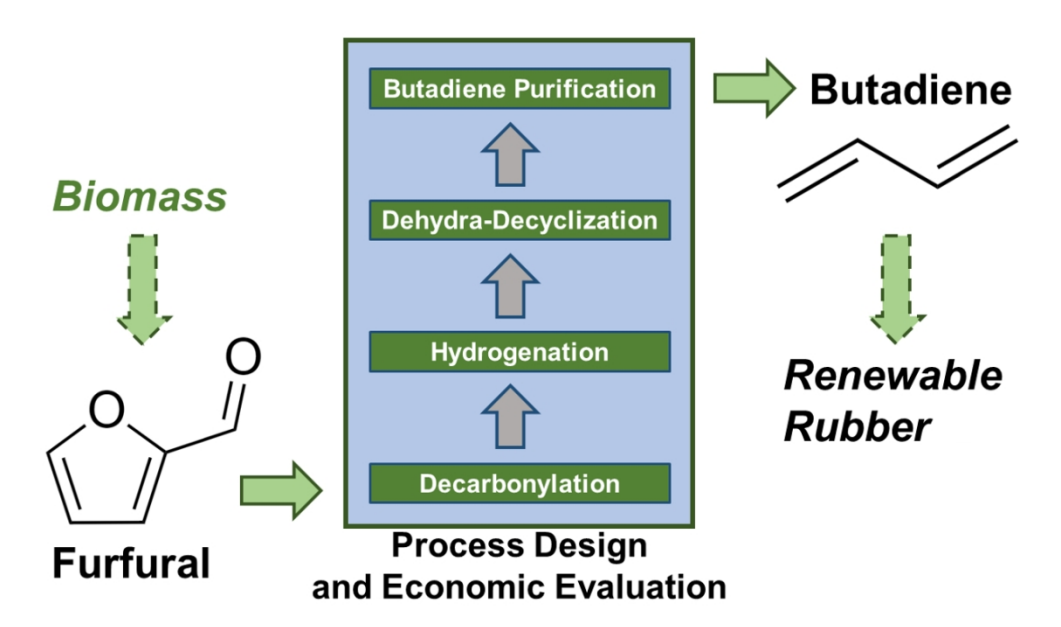


Figure 7
237x147mm (96 x 96 DPI)



Graphical Abstract - Table of Contents Graphic  $106x62mm (300 \times 300 DPI)$